Asian Journal of Green Chemistry 3 (2019) 103-124

Contents lists available at Avicenna Publishing Corporation (APC)

Asian Journal of Green Chemistry

Journal homepage: www.ajgreenchem.com

Original Research Article

Bio fabricated of silver nanoparticles using *Ocimum basilicum* and its efficacy of antimicrobial and antioxidant activity

Devan Elumalai[a,d], Manickam Sathiyaraj[b], Elangovan Vimalkumar[c], Patheri Kunyl Kaleena[d]*, Maduraiveeran Hemavathi[e], Perumal Venkatesh[b]

[a] *PG. Department of Zoology, Pachaiyappas College for Men, Kanchipuram-631 501, Tamilnadu, India*

[b] *PG & Research Department of Chemistry, Pachaiyappas College, Chennai-600 030, Tamilnadu, India*

[c] *Department of Zoology, Auxilium College (Autonomous), Gandhi Nagar, Vellore-632 006, Tamilnadu, South India*

[d] *Department of Zoology, Presidency College (Autonomous), Chennai-600 005, Tamilnadu, India*

[e] *Department of Zoology, Pachaiyappas College for Women, Kanchipuram-631 501, Tamilnadu, India*

ARTICLE INFORMATION

Received: 4 June 2018
Received in revised: 2 July 2018
Accepted: 2 July 2018
Available online: 19 August 2018

DOI: 10.22034/ajgc.2018.6729

KEYWORDS

Ocimum basilicum
Ag-NPs
Antioxidant
Antimicrobial activity

ABSTRACT

To resolve the efficacies of antibacterial, antifungal, and antioxidant activities of aqueous leaf extract of *Ocimum basilicum* mediated biosynthesis of silver nanoparticles (Ag-NPs). Aqueous and synthesized Ag-NPs were evaluated using disc diffusion method against the bacterial and fungal pathogens. Antioxidant activity of the synthesized Ag-NPs and aqueous plant extract were determined. The scavenging radicals were estimated by DPPH method. The synthesized Ag-NPs were characterized using XRD, FT-IR, FESEM, and EDX. XRD peaks at 27.6°, 32.2°, 38.16°, and 46.04° represented the (110), (111), (121), and (200) planes. FT-IR absorption peak located at 2910 cm^{-1} are due to C–H stretch of alkenes and a peak at 1669 cm^{-1} due to -C=C- band of alkenes and a peak at 1614 cm^{-1} is assigned to N-H bend of 1° amines and a peak at 1092 cm^{-1} due to C–N stretch of aliphatic amines and a peak at 875 cm^{-1} are due to C–H stretch of aromatics. The results of the TEM analysis revealed that most of the nanocrystals were spherical and polyphedral, functioning against the bacteria *Staphylococcus aureus, Escherichia coli, Klebselia pneumonia, Proteus mirabilis, and Proteus valgar*. Ag-NPs exhibited strong antibacterial activity antifungal activity versus *Asfergillus flavus, Asfergillus terreus, Asfergillus niger, Asfergillus fumigates* exhibited a 7.8, 7.5, 6.9, and 7.1 mm inhibition zone using the Ag-NPs. Green synthesized Ag-NPs provides a promising approach can satisfy the requirement of large-scale industrial production bearing the advantage of low-cost, eco-friendly and reproducible.

Corresponding author, email: drpkklab@gmail.com (P.K. Kaleena).
Fax: 044 28586401.

Graphical Abstract

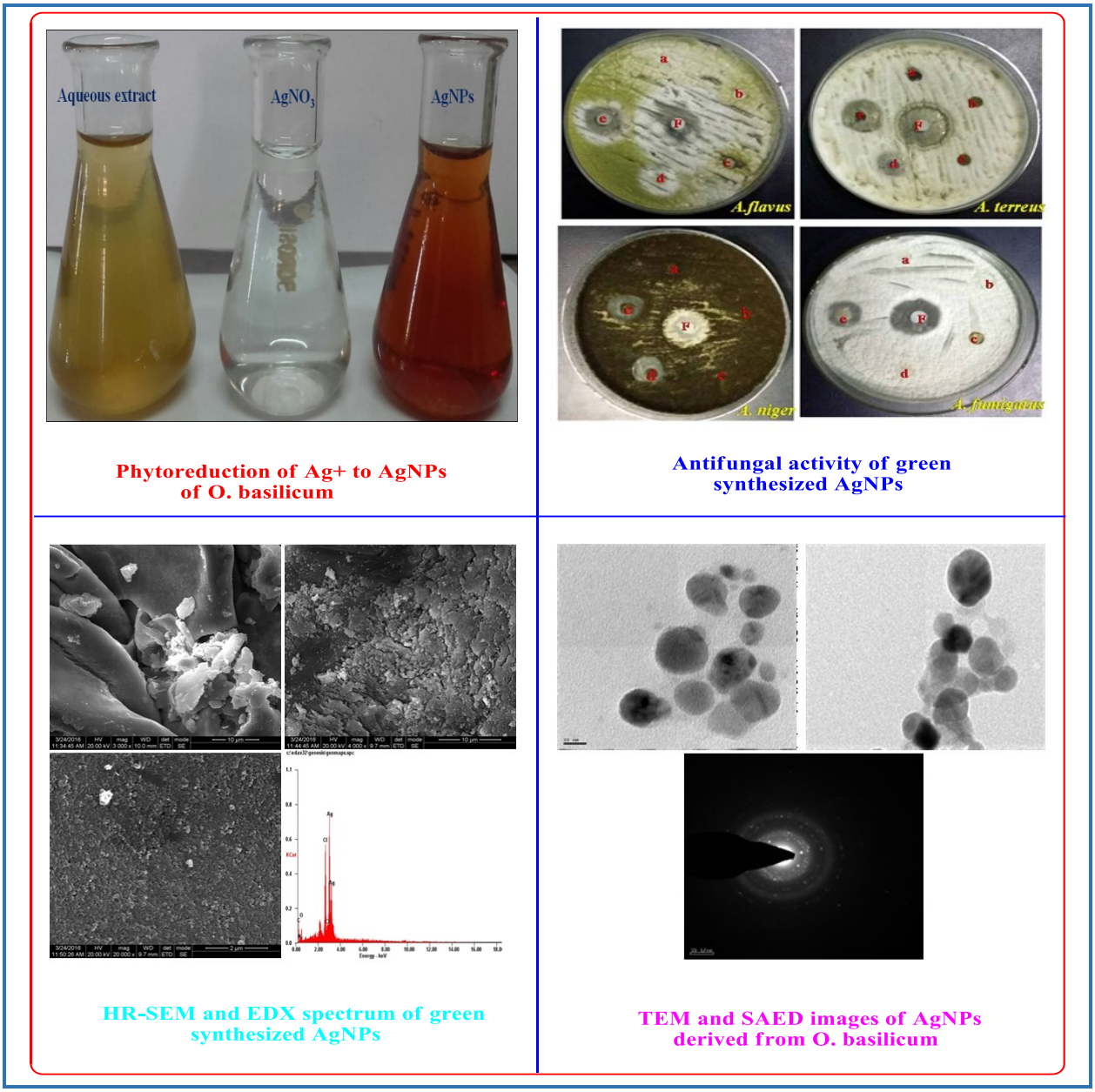

Introduction

Nanoparticle has multifunctional properties with interesting application in various field such as in medicine, nutrition, and energy [1]. Its most important application in medical industry is ointments that used against fungal or bacterial infections [2].

In recent years, Ag-NPs have been considered as a viable alternative to produce new generation of antimicrobial agents. Various chemical and physical methods have been developed to synthesize AgNPs. These methods require noxious reducing and stabilizing agents which increase the

environmental toxicity or hazardous wastes [3]. Biological methods are emerged as an alternative to the conventional methods for synthesis of NP_S synthesis of inorganic nanoparticles biological system makes nanoparticles more biocompatible and environmentally friendly [4]. The most widely followed method for the biosynthesis of nanoparticles is a type of bottom up approach where the mechanism of reaction is predominantly reduction/oxidation. Green biosynthesis of nanoparticles need for was felt as the physical and chemical processes were very expensive [5]. Recently the biosynthesis of reported successfully, these biological synthesized nanomaterials have potential application in different areas such as treatment diagnosis development surgical nanodevices and commercial product manufacturing [6]. Plants contain be explored in the synthesis of Ag-NPs due to recognized bioactive potential, particularly for their antimicrobial activity. The Ag-nanoparticles were effectively disrupting the polymer sub units of cell membrane in pathogenic organisms. The reciprocal actions of nanoparticles were subsequently breaks the cell membrane and disturb the protein synthesis mechanism in the bacterial system [7]. The fungicidal mechanisms of the biosynthesized metallic nanoparticles have a higher potential compared with that of the commercial antibiotics such as fluconazole and amphotericin. The plant derived Ag nanoparticles have clearly revealed some membrane damage in Candida sp and damage in fungal intercellular components and finally cell function was destroyed [8]. The multifunctional Ag-NPs have a promising activity against spore producing fungus and effectively destroy the fungal growth. The fungal cell membrane structure significant changes were observed by treating it with metallic nanoparticles [9].

Ocimum basilicum (Sweet basil; lamiaceae) is often used as an effective medicine all over the world [10]. In many countries, this herb is widely utilized for culinary purposes spice, flavors, essential, oil and therapeutic application [11]. The leaves and flowering parts of the *O. basilicum* are commonly used to treat fever, nausea, abdominal cramps, gastroenteritis, migrins, insomnia, depression, gonorrhea, dysentery, chronic diarrhea, and exhaustion. External applications include treatment of acne, loss of smell, insect stings, snake bites and skin infection [12]. More importantly, have been identified for its profound anti-lipidemic, anti-cholesterol, anti-microbial and anti-diabetic properties [13]. Safety, therapeutic effectiveness, economic benefits and availability are important advantages that *O. bacilicum* possess [14], *Swarnalatha* et al. [15] provide a natural source of anti-oxidants capable of neutralizing free radical and reducing the severity of diabetic micro and macrovascular complications. The present investigation was made to synthesis sliver nanoparticles be using the leaf extract of *O. basilicum* to find their antimicrobial activity on selected microorganisms.

Experimental

Materials and methods

Plant collection

Ocimum basilicum weeds are found growing as dense clumps along the roadsides of Kanchipuram, Tamilnadu, India. *O. basilicum* (Figure 1) were identified was made by *Dr. P. Paramasivam*, Department of Botany, Pachaiyappas College for Men, Kanchipuram. The voucher 2012 specimen was numbered and deposited in our botany herbarium.

Preparation of plant extract

The leaves of *O. basilicum* were washed with tap water for 10 min to remove the dust particles and rinsed briefly in deionized water. The aqueous solution was prepared by taking 8 gr of washed and finely cut leaves in a 250 mL erlenmeyer flask along with 100 mL of deionized water and the mixture was boiled at 60 °C for 20 min. This extract was filtered through nylon mesh (Spectrum), followed by millipore hydrophilic filter (0.22 m) and used for further experiments [16].

Synthesis of silver nanoparticles

Fresh extract was used for the reduction of Ag^{+} ions to Ag^{o}, where in 4 mL of extract was added to 96 mL of aqueous silver nitrate (1 mM) solution and incubated at 28 °C for 60 min. The bio-reduced Ag-NPs were analyzed using UV-visible spectroscopy.

Figure 1. *Ocimum basilicum*

Antioxidant activity

Antioxidant property of the leaf extract was determined by DPPH assay [17]. The free radical scavenging ability of the extracts against DPPH free radical was evaluated. 1 mL of 0.1 mM DPPH in ethanol was prepared. To that prepared solution plant extracts varying in concentrations from 100–1000 µg/mL, 1 mL ethanol and 0.95 mL Tris HCl were added. The mixture was left 30 minute and the absorbance was measured at 517 nm. The DPPH free radical scavenging activity was subsequently calculated.

$$\% \text{ DPPH radical scavenging} = \frac{\text{Control OD}}{\text{Control OD} - \text{sample OD}} \times 100$$

UV- visible spectral analysis

1 mL of sample was withdrawn at time intervals and surface plasmon resonance of silver nanoparticles was characterized using a UV-vis spectrophotometer (Shimadzu 1601 model, Japan) at a resolution of 1 nm between 200 to 800 nm. Furthermore, the final nano-colloidal solution was subjected to repeated centrifugation (Twice) to get rid of any un-interacted biological molecules at 10,000 rpm for 20 min in Remi Research Centrifuge. The final pellet was collected, dried in vacuum desiccators and stored for future use. From the synthesized NPs different test concentrations of aqueous solutions were prepared.

Fourier transform infrared (FT-IR) spectroscopy

For FT-IR analysis, the powdered sample of the Ag-NPs was prepared by centrifuging the synthesized Ag-NPs solution at 10,000 rpm for 20 min. The solid residue obtained was then washed with deionized water to remove any unattached biological moieties to the surface of the nano-particles, which are not responsible for biofunctionalization and capping. The resultant residue is then dried completely and the powder obtained is used for FT-IR measurements to obtain an idea about the chemical framework around the formed nanoparticles by a FT-IR Spectrometer (PERKIN ELMER-SPECTRUM ONE). The scanning range was 4000–450 cm^{-1} at a resolution of 4 cm^{-1}.

X-ray Diffraction (XRD) Analysis

The formation and quality of compounds were checked using X'Pert Pro Materials Research diffractometer system. The x-ray diffraction (XRD) pattern was measured by drop coated films of $AgNO_3$ on glass plate and employed with characteristic radiation in the range of 20–90° at a scan rate of 0.05°/min with the time constant of 2 s, CuKα radiation and amplitude wave k=1.5418 Å working with a 40 kV voltage and 30 mA current. The full-width at half-maximum (FWHM) from

three different peaks were used in Scherrer's equation to determine the average crystallite size of the nanoparticles.

High resonance scanning electron microscope (HRSEM) analysis

Morphological analysis was conducted using Hitachi SU6600 HR-SEM machine. Thin film samples were prepared on a carbon coated copper grid by just dropping a very small amount on the grid, extra solution was removed using a blotting paper and then the films on the SEM grid were allowed to dry by placing it under the mercury l amp for 5 min.

High resonance-transmission electron microscopy (HRTEM) of silver nanoparticles

The transmission electron microscopy (TEM) images were obtained using JEOL model 3010 instrument operated at 200 kV and a beam current of 104.1 μA. Sample for this analysis were prepared by coating the aqueous Ag-NPs on carbon coated copper grids (300 mesh size) by slow evaporation and then allowed to dry in vacuum at 25 °C for overnight.

Antimicrobial assay

The antibacterial activity of green synthesized Ag-NPs was tested against five bacterial isolates such as Staphylococcus aureus, Escherichia coli, Klebselia pneumonia, Proteus mirabilis, Proteus valgaris and Sabouraud dextrose agar (SDA) was prepared according to specifications, autoclaved (121 °C for 15 min) and dispensed into petridishes. Asfergillus flavus, Asfergillus terreus, Asfergillus niger, Asfergillus fumigates using Agar disk diffusion method [18]. Nutrient Agar plates were inoculated with 100 μL of standardized culture (1.5×108 CFU/mL) of each bacterium (intriplicates) and spread with sterile swabs. Wells of 6 mm size are made in the Agar plates containing the bacterial lawn. From the synthesized Ag-NPs, 5, 10, 15, 20, and 25 μg/μl volume were poured into the wells made in the bacterial culture plates. The plates thus prepared were left at room temperature for ten minutes for allowing the diffusion of the extract into the agar bacterial lawn. After incubation for 24 h at 37 °C, the plates were observed. The zone of inhibition was measured and expressed in millimeters.

Results and discussion

Preliminary screening of active phytochemicals

Preliminary phytochemical screening of revealed the *O. basilicum* presence of phytochemicals such as tannins, alkaloids, carbohydrates, cardiac glycosides, flavonoids, phenols, saponins,

steroids, terpenoids and triterpenoid. Quinones, cumarins, cyanin and glycosides are absent (Table 1).

UV–vis analysis of phyto-synthesised solutions

The aqueous extracts of *O. basilicum* when mixed in aqueous solution of silver ion complex, the reduction of pure Ag^{+} ions to Ag^{o} was monitored by measuring UV-vis spectrum of the reaction media. The reduction of silver nitrate into Ag-NPs during exposure to plant extract is followed by a gradual increase in color development from clear to yellowish brown, as a result of the surface plasmon resonance (SPR) phenomenon (Figure 2).

The UV-visible spectral analysis of plant extracts without $AgNO_3$ did not show any change in color. The UV-vis spectra of all the samples exhibited distinct surface plasmon resonance bands (SPR). The position of SPR band in UV-vis spectra is sensitive to particle shape, size, its interaction with the medium, local refractive index and the extent of charge transfer between medium and the particles. Here, the sharp bands were centered at 450 nm in *O. basilicum* synthesized Ag-NPs extracts clearly indicate the presence of silver nanoparticles (Figure 3).

FT-IR analysis of synthesized silver nanoparticles

FT-IR spectroscopy is used to probe the chemical composition of the surface of the silver nanoparticles and to identify the possible biomolecules responsible for the reduction of the Ag^{+} ions and the capping of the bioreduced silver nanoparticle synthesized by the leaf extracts. The FT-IR spectrum of *O. basilicum* extracts mediated silver nanoparticles are shown in (Figure 4). The FT-IR spectrum of *O. basilicum* leaf extracts mediated Ag-NPs showed bands at 3402 cm^{-1} which is assigned to O–H stretching vibration of phenolic and alcoholic compounds. The medium absorption peak located at 2910 cm^{-1} are due to C–H stretch of alkenes and a peak at 1669 cm^{-1} due to -C=C- band of alkenes and a peak at 1614 cm^{-1} is assigned to N–H bend of 1° amines and a peak at 1092 cm^{-1} due to C–N stretch of aliphatic amines and a peak at 875 cm^{-1} are due to C–H stretch of aromatics.

X- ray diffraction (XRD) of synthesized silver nanoparticles

X-ray diffraction analysis was used to confirm the crystalline nature of the particles (Figure 5) shows a representative XRD pattern of the silver nanoparticles synthesized by *O. basilicum* leaf extract after complete reduction of silver. The XRD pattern showed numbers of Bragg reflections that may be indexed on the basis of the face-centered cubic structure of silver. A comparison of the XRD spectrum with the standard confirmed that the silver particles formed were in the form of

nanocrystals, as evidenced by the peaks at 2θ values of 27.6°, 32.2°, 38.16° and, 46.04° representing the (110), (111), (121), and (200) Bragg's reflections which may be indexed based on the face-centered cubic structure of metallic silver. The XRD results revealed that the silver nanoparticles formed by the reduction of Ag^+ ions by the *O. basilicum* leaf extract are crystalline in nature.

Table 1. Phytochemical screening of aqueous leaf extract of the *O. basilicum*

S.No	Secondary metabolite	Aqueous extract
1	Carbohydrates	Strongly positive
2	Tannins	Positive
3	Saponins	Strongly positive
4	Flavonoids	Positive
5	Alkaloids	Positive
6	Quinones	Not detected
7	Glycosides	Not detected
8	Terpenoids	Trace
9	Triterpenoids	Positive
10	Phenols	Positive
11	Cumarins	Strongly positive
12	Acids	Not detected
13	Protein	Not detected
14	Cyanin	Positive
15	Cardiac glycosides	Positive

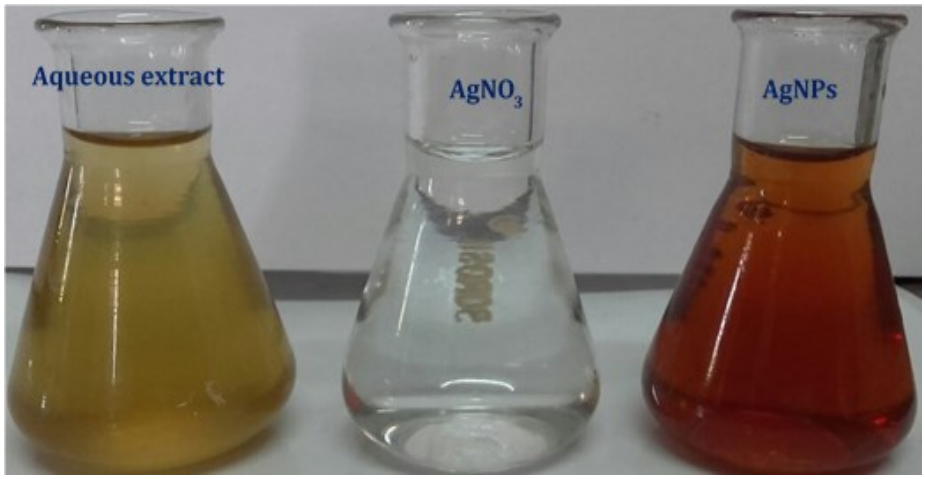

Figure 2. Shows colour change from light yellow to brown before and after the process of phytoreduction of Ag+ to Ag-NPs of *O. basilicum*

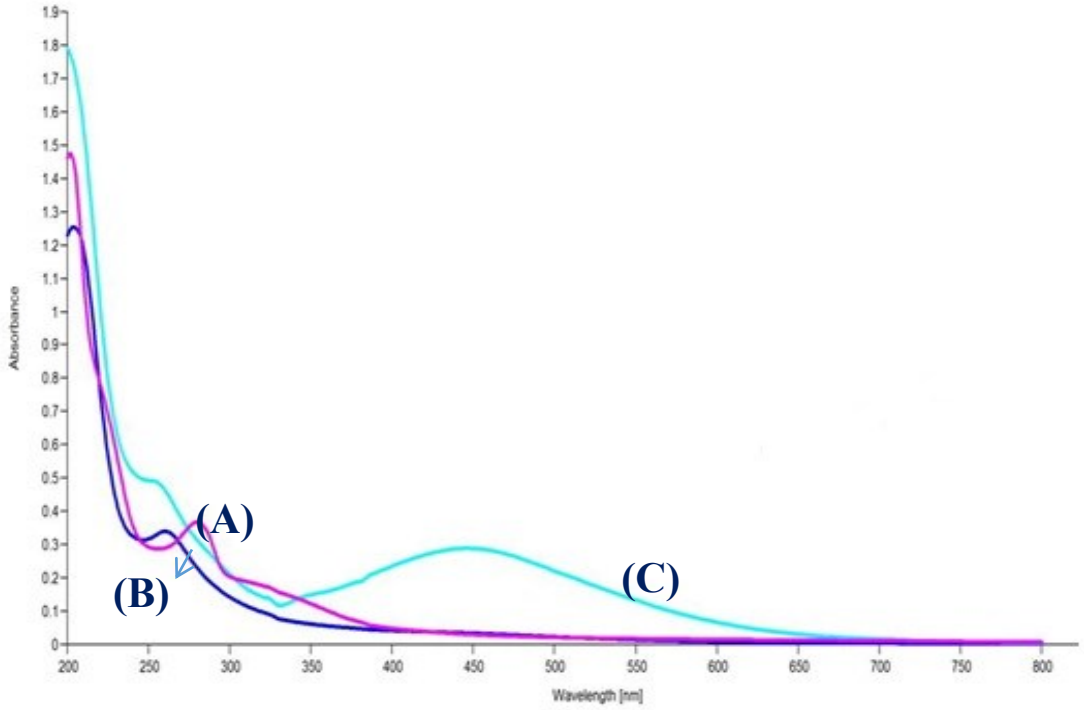

Figure 3. UV-visible spectrum of a) aqueous extract, b) silver nitrate solution and c) green synthesized Ag-NPs

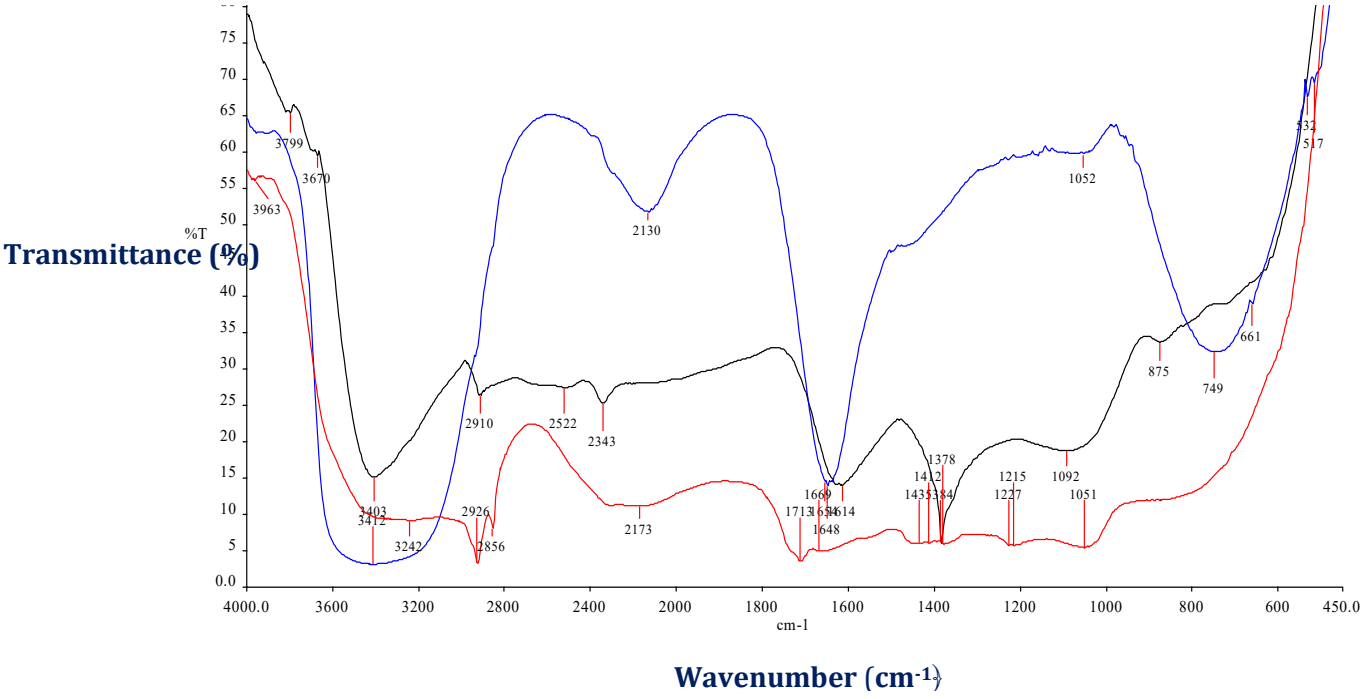

Figure 4. FT-IR spectrums of *O. basilicum* leaf extract, silvernitrate and green synthesized Ag-NPs

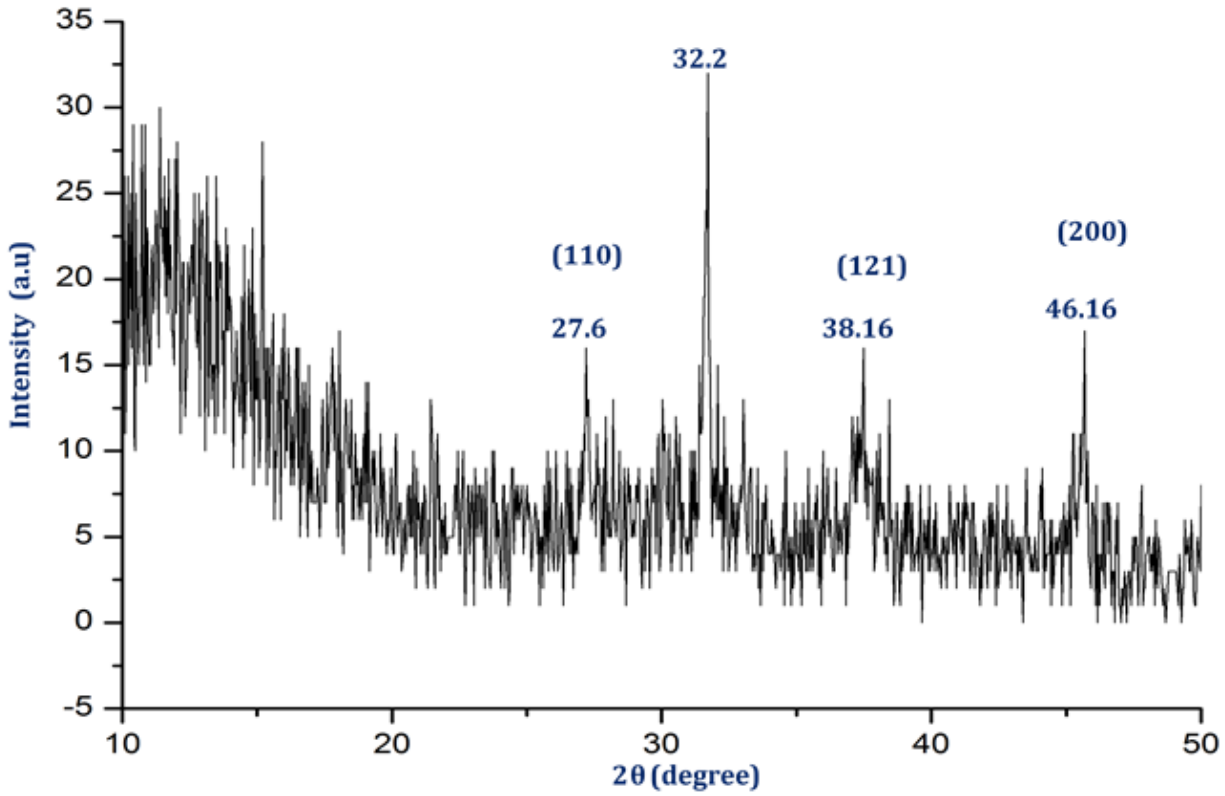

Figure 5. XRD pattern of green synthesized Ag-NPs from aqueous leaf extract of *O. basilicum*

SEM analysis of synthesized silver nanoparticles

While the absorption spectra provided solid evidence of nanoparticle formation and their growth kinetics, the surface morphology of the nanoparticles were characterized by SEM (Figure 6). The SEM images indicated the clustered nature and the particles were prominently cuboidal and a few were spherical in shape. Magnified SEM image confirms that the silver nanocubes are in well resolved cuboidal structure with soft surface and with sharp edges.

EDX profile of synthesized silver nanoparticles

The synthesis of silver nanoparticles from *O. basilicum* was further characterized by EDX analysis, which gives additional evidence for the reduction of silver nanoparticles to elemental silver (Figure 7). The optical absorption peak is seen approximately at 3 keV, which is typical for the absorption of metallic silver nanocrystals due to surface plasma resonance, which confirms the presence of nanocrystalline elemental silver. The spectrum shows strong silver signal along with weak oxygen and carbon peak, which may be originating from the biomolecules that are bound to the surface of the silver nanoparticles.

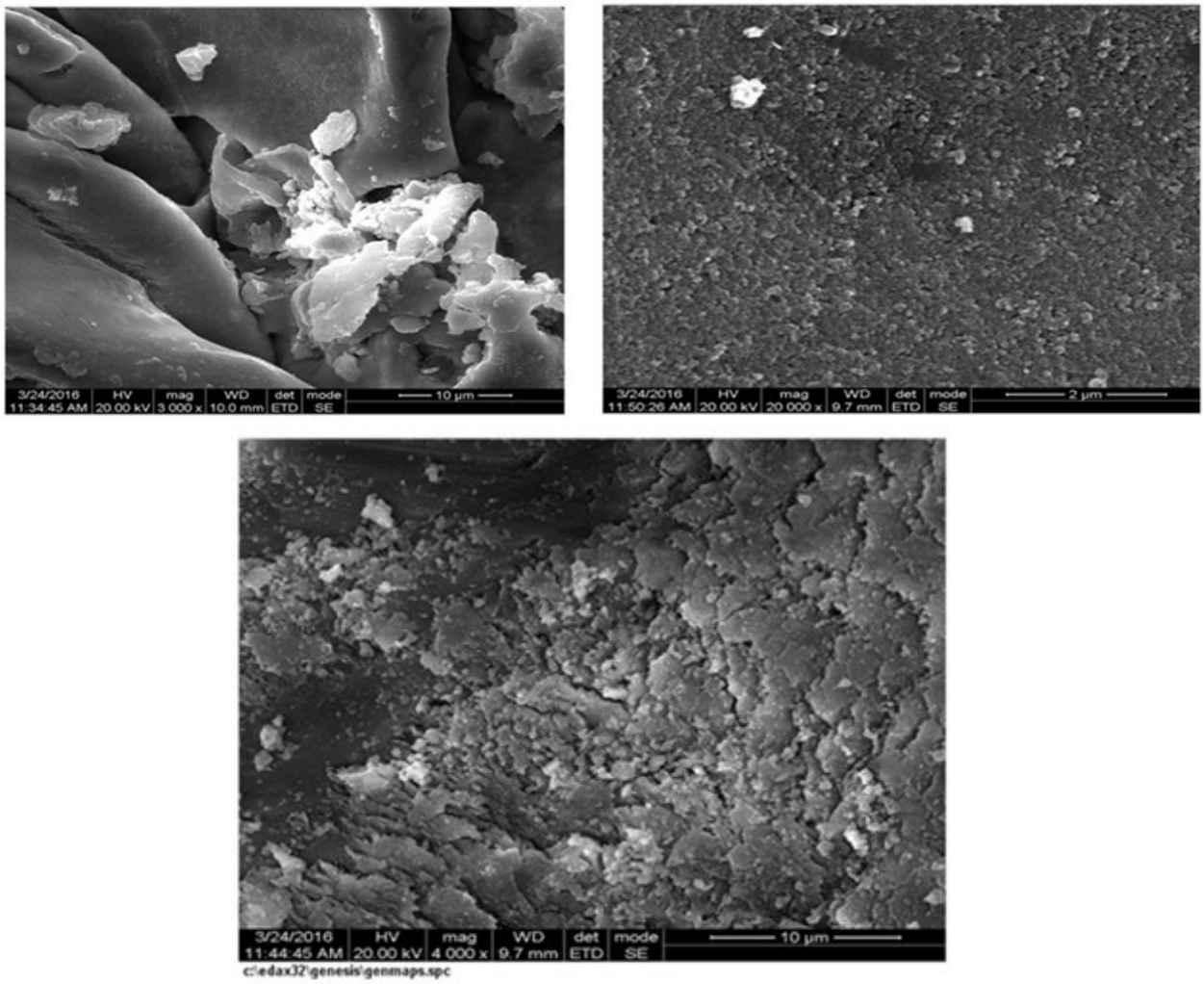

Figure 6. HR-SEM images of green synthesized Ag-NP

Figure 7. EDX spectrum of green synthesized Ag-NP

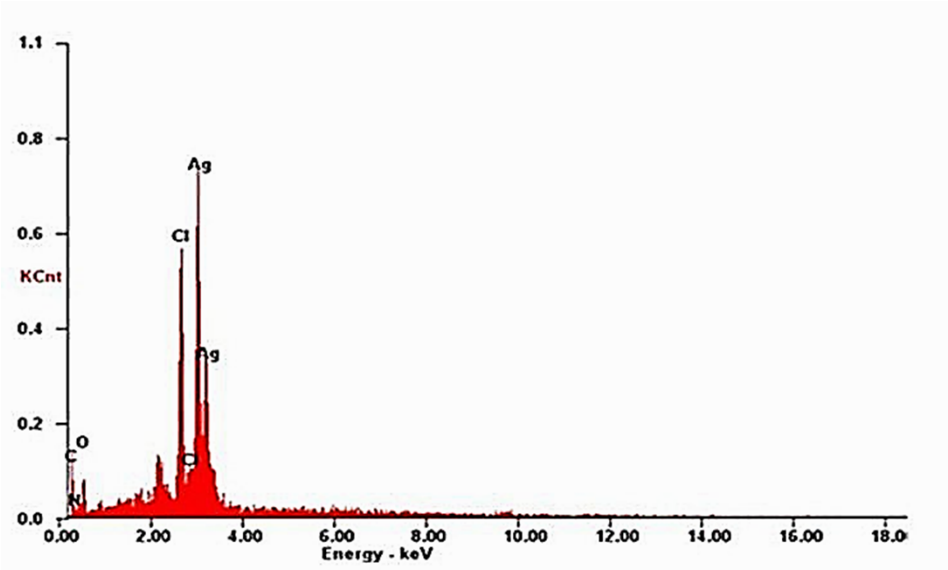

TEM analysis of synthesized silver nanoparticles

The size and morphology of Ag-NPs were determined by transmission electron microscopy (TEM) images. TEM was employed to analyze the size and the shape of the biogenically stabilized Ag nanoclusters shows that most of the nano-crystals formed from *O. basilicum* leaf extract are spherical in shape, largely uniform with a moderate variation in particle size. According to size distribution, most of nanoparticles ranged from 20 to 50 nm. Furthermore, the SAED pattern proved that the green silver NPs are single crystalline in nature (Figure 8). Selected area electron diffraction (SAED) pattern of one the spherical particles indicates the fececentred (fcc) crystalline nature of the nanoscale particles. The study reveals that most of the nanocrystals formed were spherical and polyphedral in shape. The crystal lattice planes with ordered orientation of the lattice fringes are literally visible in one of the particle image.

Antioxidant activity of Ag nanoparticles

Antioxidant activity of Ag nanoparticles was assessed by DPPH free radical scavenging assay. DPPH is a stable compound and accepts hydrogen or electrons from silver nanoparticles. The results obtained in the antioxidant assay showed effective free radical scavenging b Ag nanoparticles (Figure 9). The antioxidant potential of silver nanoparticles could be attributed by functional groups adhere to nanoparticles from leaf extract.

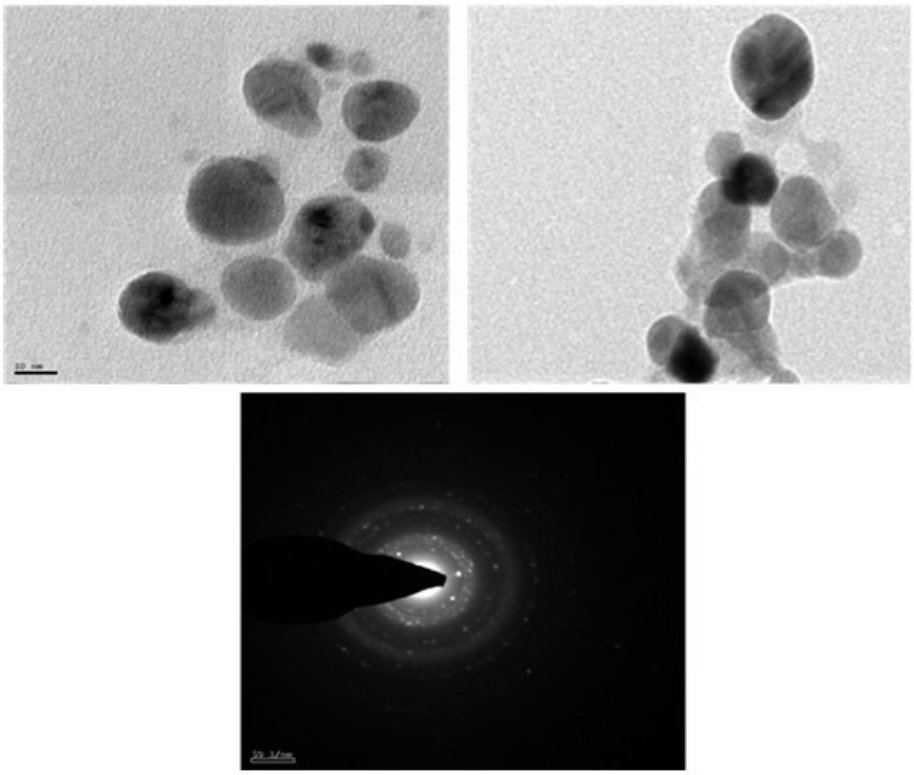

Figure 8. TEM and SAED images of Ag-NPs derived from *O. basilicum*

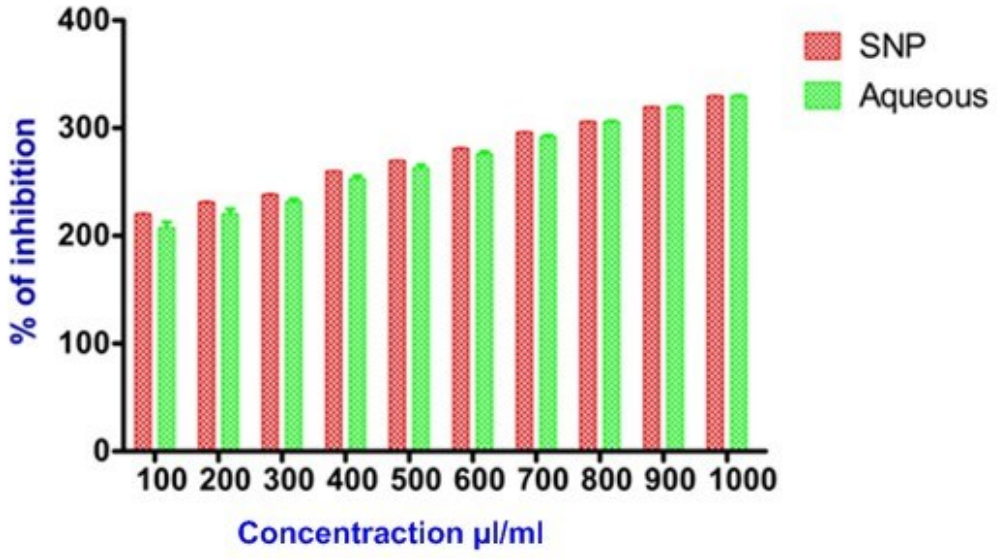

Figure 9. Antioxidant activity of silver nanoparticles

Antimicrobial activity of silver nanoparticles

Antimicrobial activity of silver nanoparticles was tested against laboratory test organism of biological importance, i.e., *Staphylococcus aureus*, *Escherichia coli*, *Klebselia pneumonia*, *Proteus mirabilis*, *Proteus valgaris*, *Asfergillus flavus*, *Asfergillus terreus*, *Asfergillus niger*, and *Asfergillus fumigates*. The antibacterial potential of silver is well known. The synthesized Ag-NPs were tested for their antibacterial action (Table 2 and 3). The *O. basilicum* aqueous leaf extract of the inflorescence and silver nitrate were also tested separately for antibacterial activity. Bioreduced silver nanoparticles showed a higher antibacterial activity than the aqueous leaf extract. Figure 10 and 11 demonstrates the photographs taken after antimicrobial measurements. The image show 8.9, 9.2, 7.8, 8.1, and 7.4 mm inhibition zones against the bacteria *S. aureus, E. coli*, *K. pneumonia*, *P. mirabilis*, and *P. valgaris* using the nanoparticles as antibiotics. The inhibition zone is clear in both cases, which show that silver nanoparticles exhibited strong antibacterial activity against *S. aureus*, *E. coli*, *K. pneumonia*, *P. mirabilis*, and *P. valgaris* prohibit their proliferation.

The study of antifungal activity versus *A. flavus*, *A. terreus*, *A. niger*, *A. fumigates* exhibited a 7.8, 7.5, 6.9 and 7.1 mm inhibition zone using the silver nanoparticles (Figure 12 and 13). The inhibition zone against A. *flavus*, *A. terreus*, *A. niger*, *A. fumigates* reveals that was prevented at different concentration of 5, 10, 15, 20, and 25 $\mu g/\mu l$ of silver nanoparticles (Table 4). A Norflaxin disc was used as a positive control. *O. basilicum* leaf aqueous extract alone did not show any activity against pathogens. The antimicrobial activity of silver nanoparticles depends on their shape and size. These results showed that the nanoparticles exhibited good activity against gram positive and gram

negative bacteria and fungi. Thus, the nanoparticles may be considered as a desired antibiotic and antifungal material.

Several approaches have been employed to obtain a better synthesis of Ag-NPs such as chemical and biological methods. Recent reports on biological synthesis of Ag-NPs revealed nanobiotechnological potential of several pharmacologically important plant materials have been successfully explored for metal nanoparticle synthesis. Several products from biological origins were useful surviving humanity and its associated life in various aspects like drug development and nutritional adequate. Particularly plant is the warehouse several bioactive compounds, the interaction between plant biochemical and inorganic nanoparticles tend to be hopeful area in nanoscience and technology. The DPPH free radical scavenging assay showed potent inhibitory capacity for the synthesized silver nanoparticles. The percentage of inhibition increased with increase in concentration of silver nanoparticles. Similar observations with enhanced DPPH scavenging activity by selenium, platinum, silver nanoparticles [19].

The antioxidant property has been proved by some researches to be related with the development of reducing power. Reductones, which have strong reducing power, are generally believed not only to react directly with peroxides but also to prevent peroxide formation by reacting with certain precursors [20].

UV–visible spectra of the mixture of Ag-NPs -$AgNO_3$ solution were recorded against time of reaction. UV-visible spectroscopy is a widely used technique for structural characterization of silver nanoparticles [21]. Generally, the results of the UV-visible absorption showed increasing color intensity with increased time intervals and this might be due to the production of the nanoparticles [22]. The color of the solution that gradually turned from light yellow into brown in, 1 h indicates the formation of Ag-NPs. The appearance of the brown color was due to the excitation of the surface plasmon vibrations. The formation of Ag-NPs was monitored by UV-visible spectroscopy in 200–800 in range. Typically, the synthesized Ag-NPs are having λ max values which are in the visible range 400–500 nm.

Recently several approaches have been reported to synthesize Ag-NPs in smarter ways which include both chemical and biological approaches [23]. According to green chemistry principles, now a day using bio-based matter in synthesizing material is of great interest to the scientific community. In comparison with chemical approaches bio-based approaches were fast and smart enough against uses at foxic and hazardomchemicob and byproducts. In this context the present study used *O. basilicum* aqueous extract to synthesize Ag-NPs which is rich in polyphenolic contents.

Table 2. Antibacterial activity of leaf aqueous extract of *O. basilicum* against human pathogens

S.No	Name of the bacteria	Zone of inhibition in mm						
		5 µg/µl	10 µg/µl	15 µg/µl	20 µg/µl	25 µg/µl	30 µg/µl	Norflaxin 20 µg/µl
1	*Staphylococcus aureus*	7.2	7.8	7.9	8.5	8.6	8.2	12
2	*Escherichia coli*	0	0	0	6.8	6.9	7.3	11
3	*Klebselia pneumonia*	0	6.5	6.8	6.9	7.2	7.5	13
4	*Proteus mirabilis*	0	0	0	0	6.7	7.1	9.3
5	*Proteus valgaris*	0	0	0	6.3	6.7	6.9	8.6

Table 3. Antibacterial activity of Ag-NPs against human pathogens

S.No	Name of the bacteria	Zone of inhibition in mm						
		5 µg/µl	10 µg/µl	15 µg/µl	20 µg/µl	25 µg/µl	30 µg/µl	Norflaxin 20 µg/µl
1	*Staphylococcus aureus*	7.2	7.8	7.9	8.5	8.6	8.2	12
2	*Escherichia coli*	0	0	0	6.8	6.9	7.3	11
3	*Klebselia pneumonia*	0	6.5	6.8	6.9	7.2	7.5	13
4	*Proteus mirabilis*	0	0	0	0	6.7	7.1	9.3
5	*Proteus valgaris*	0	0	0	6.3	6.7	6.9	8.6

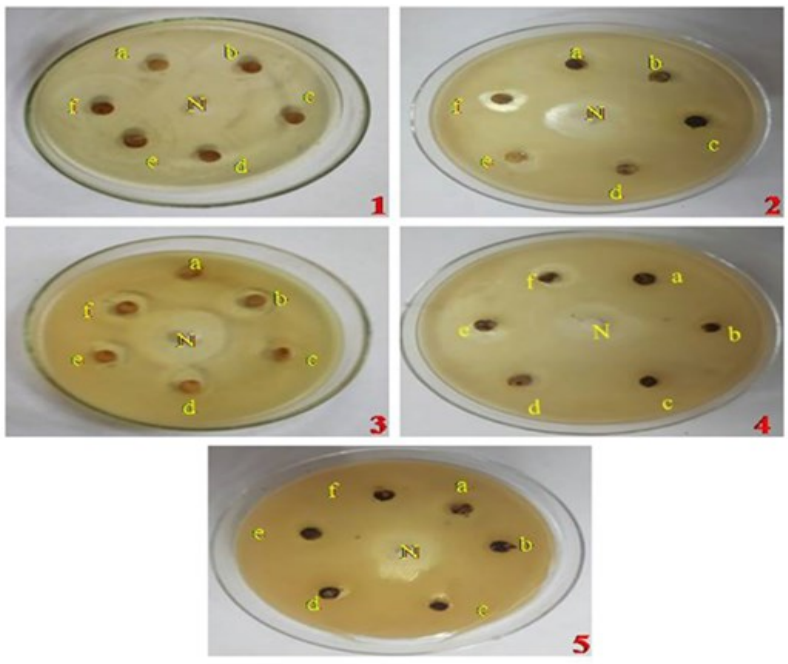

Figure 10. Antibacterial activity of leaf aqueous extract of *O. basilicum* against 1) *S. aureus*, 2) *E.coli*, 3) *K. pneumonia*, 4) *P. mirabilis*, and 5) *P. valgaris*

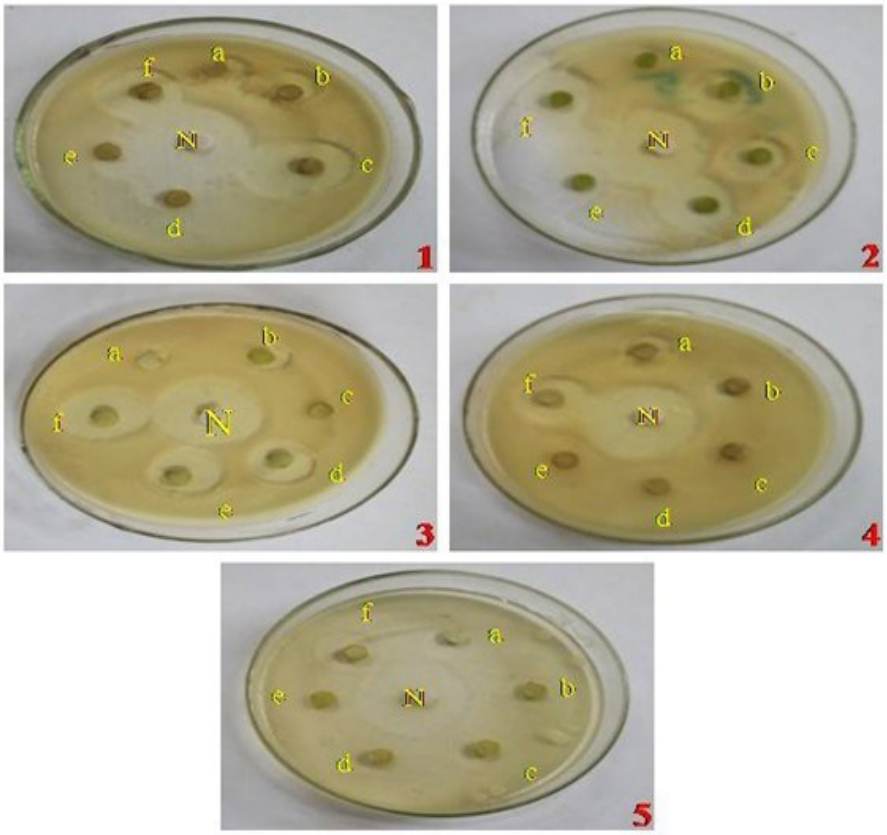

Figurer 11. Antibacterial activity of green synthesized Ag-NPs against 1) *S. aureus,* 2) *E. coli,* 3) *K. pneumonia,* 4) *P. mirabilis* and 5) *P. valgaris*

FT-IR analysis was conducted to identify the possible interactions between silver and bioactive molecules, which may be responsible for synthesis and stabilization (Capping) of silver nanoparticles. The prominent peaks in the FT-IR results show the corresponding values in the amide group (N–H stretching 3416 cm^{-1}), alkane group (C–H stretching 2921 cm^{-1}), respectively. *Asmathunisha* et al [24] reported that the observed peaks of amide and aromatic rings are considered on functional groups of flavonoids, triterpenoid, and polyphenols. The linkage of metal ions and the amide group (Containing enzymes) of plant biomoleculos is responsible for the reduction, synthesis and stabilization of the metal ions as well as the amine containing organists (polyphenols) having good potential reducing against in the synthesis of silver nanoparticles [25]. The absorption bands located at 1376 and 1008 cm^{-1} may be attributed to C–O and C–O–C stretching modes. The medium intense band at 1464 cm^{-1} arises from the C–N stretching mode to the aromatic amine group [26]. The peak at 1644.9 cm^{-1} refers to the C=C stretch vibration of primary alkenes. FT-IR spectrum of the most intense band at 1620–1636 cm^{-1} represents carbonyl groups from polyphenols such an, gallocatechin gallate and the aflavin; the results suggest that

molecules attached with Ag-NPs have free and bound amide groups. These amide groups may also be in the aromatic rings. So, the compounds attached with the Ag-NPs could be polyphenols with an aromatic ring and bound amide region [27]. The carbonyl groups of the amino acid residues and the peptides have strong ability to bind to the silver. It is also reported that the proteins can bind to nanoparticles either through free amine or cysteine groups in proteins [28]. The FT-IR spectral analysis confirms the presence of organic molecules such an ethylamine, alkanes, alkenes, amines-primary, nitrogroups, ester, and confirms that *O. bascilicum* plant extract plays an important role in the green synthesis of Ag-NPs.

XRD analysis of the nanoparticles showed intense peak corresponding to (110), (111), (121), and (200) Bragg's reflections which may be indexed based on the face-centered cubic structure of metallic silver. The broadening of Bragg's peak indicates the formation of nanoparticles. Intense Bragg's reflection suggests that strong x-ray scattering centers in the crystalline space could be due to capping agent. Therefore, XRD results suggest that crystallization of the bioorganic phase occurs on the surface of silver nanoparticles. The XRD pattern showed intense peak in whole spectrum of 2θ values ranging from 27° to 50°. A few unassigned peaks were also noticed in the vicinity of the characteristic peak. Thus, the XRD spectrum confirmed the formation of silver nanoparticles [29]. The XRD studies also suggest that crystallization of the bioorganic phase occurs on the surface the silver nanoparticles [30].

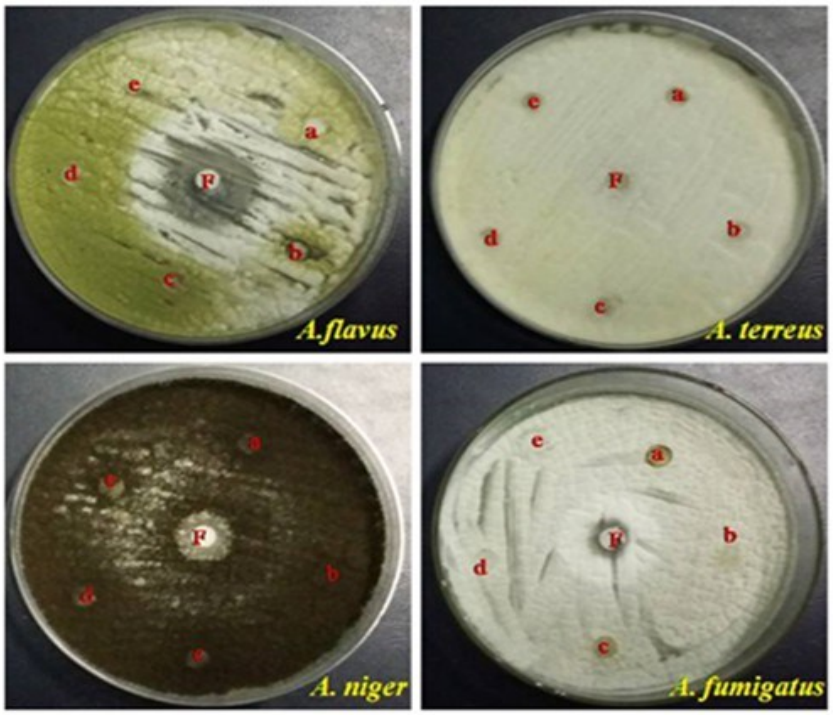

Figure 12. Antifungal activity of leaf aqueous extract of *O. basilicum A. flavus*, *A. terreus*, *A. niger*and *A. fumigates*

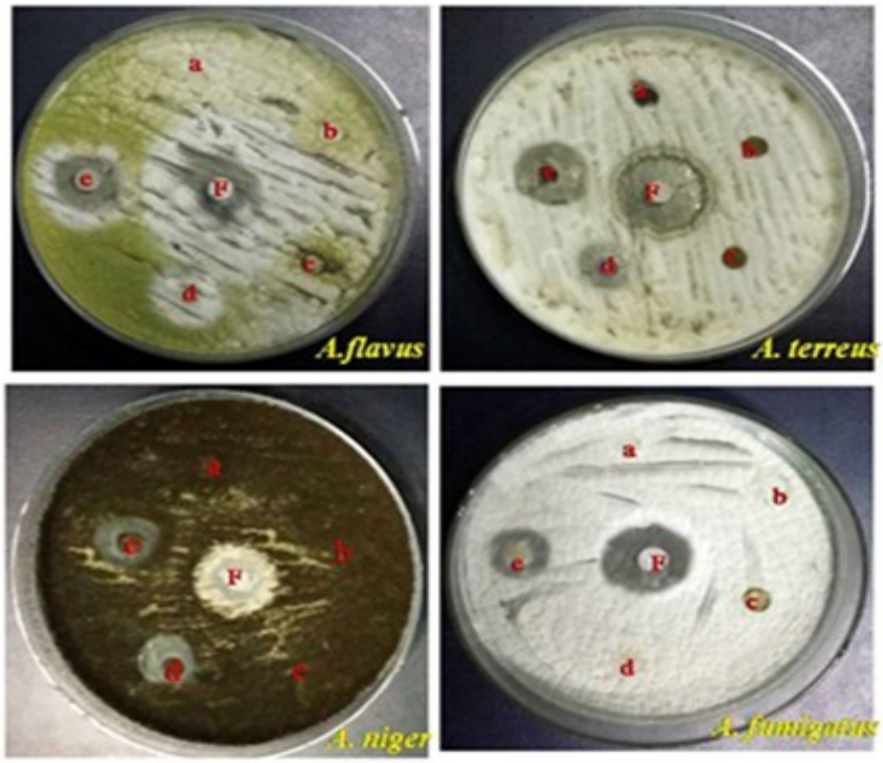

Figure 13. Antifungal activity of green synthesized Ag-NPs against *A. flavus, A. terreus, A. niger*and *A. fumigates*

Table 4. Antifungal activity of Ag-NPs against *A. flavus, A. terreus, A. niger, A. fumigates*

S.No	Name of the Fungi	Zone of inhibition in mm					
		5 µg/µl	10 µg/µl	15 µg/µl	20 µg/µl	25 µg/µl	Flucanazole
1	*A. Flavus*	0	0	0	6.5	7.8	9.1
2	*A. terreus*	0	0	0	6.3	7.5	8.3
3	*A. niger*	0	0	0	6.5	6.9	7.8
4	*A. fumigatus*	0	0	0	0	7.1	7.9

The SEM images indicated the clustered nature and the particles were prominently cuboidal and a few were spherical in shape. Magnified SEM image confirms that the silver nanocubes are in well resolved cuboidal structure with soft surface and with sharp edges. Such cuboidal nanoparticles have been reported by *Vivek* [31]. It is known that the shape of metal nanoparticle considerably change their optical and elemental properties [32].

The synthesis of silver nanoparticles from *O. basilicum* was further characterized by EDX analysis, which gives additional evidence for the reduction of silver nanoparticles to elemental silver. The spectrum shows strong silver signal along with weak oxygen and carbon peak, which may be originating from the biomolecules that are bound to the surface of the silver nanoparticles. Thus the EDX provides chemical purity of the synthesized nanoparticles [33].

The size, shape and morphology of the silver nanoparticles were studied by the transmission electron microscopy images. The grid used in the HR-TEM was prepared by placing a drop of the bioreduced diluted solution on a carbon-coated confirmed that the biosynthesized silver nanoparticles were in the size of 20 nm. The shape of the nanoparticles was analyzed as spherical and few of the Ag-NPs were agglomerated. The energy dispersive spectrum revealed that the clear identification of the elemental composition is present in the synthesized nanoparticles, which suggest the presence of silver as the ingredient element. Silver nanoparticles show an optical absorption peak at 3 keV due to the surface plasmon resonance [34]. In the earlier report of [35] the particle shape of plant–mediated Ag-NPs were mostly spherical with exception of neem (Azardirachta Indian) which yield polydispersed particle with spherical and flat plate like morphology ranging from 20 nm. In our study silver nanoparticles showed activity against *Staphylococcus aureus*, *Escherichia coli*, *Klebselia pneumonia*, *Proteus mirabilis*, *Proteus valgaris* and *A. flavus*, *A. terreus*, *A. niger*, *A. fumigates*. *Kim* et al. [36] reported that Ag-NPs showed potent activity antifungal effects, probably through destruction of membrane integrity. The mechanism of the antimicrobial effect is not very clear but some researchers have proposed that either silver ions or the nanoparticles attach to the cell wall, causing the accumulation on envelop protein precursors which result in dissipation of the proton motive force [37].

The antibacterial activity was examined by comparing colony-forming capability of different bacteria treated by various concentrations of Ag-NPs. Antibacterial activity is studied qualitatively by agar medium by well diffusion and auantitativelyinterms of the MIC. *Luo* et al. [38] had reported that the nanoparticles induce oxidative stress to bacteria and induce; normal circumstances cells are able to defend themselves against ROS damage with antioxidant enzymes. But when the nanoparticles are inside the cell, the nanoparticles could restrain antioxidative enzymes to inhibit the capability of removing ROS. *Priester* et al. [39] also reported that the nanoparticles break the balance of oxidant/ antioxidant and generate the accumulation of ROS in bacteria. It has also been reported that when silver nanoparticles are attached to the surface of cell membrane, the respiratory function and permeability of the bacterial cell become unstable. Other studies suggest that when bacteria are treated with silver ions, DNA tends to lose its ability to replicate. However extract mechanism of Ag-NPs on different bacterial cells needs a further study.

Conclusion

This study proved the ability of *O. basilicum* plant extracts to reduce Ag^{+} to Ag^{o}, the ingredients of these leaf extract acting as reducing agents for Ag^{+} as well as capping agents for phytosynthesized Ag-NPs. Furthermore, the silver nanoparticles were found to have significant DPPH free radical scavenging properties which make them to be an eco-friendly for electronic applications, cancer treatment, sensors, drug delivery, and other medical applications. In addition, the outcomes of this study illustrate a wide range of applications of electrochemically and bioactive silver nanoparticles.

Acknowledgments

The authors would like to appreciate the Principal, Pachaiyappa's College for Men, Kanchipuram, for providing infrastructure and research facilities.

Disclosure statement

No potential conflict of interest was reported by the authors.

References

[1]. Chandran S.P., Chaudhary M., Pasricha R., Ahamad A, Sastry M. *Biotechnol. Prog*., 2006, **22**:577

[2]. Shinde S., Grampurohit N., Gaikwad D., Jadhav S., Gadhave M., Shelke P., *Asian Pac. J. Trop. Biomed*., 2012, **2**:334

[3]. Amooaghaie R., Saeri M.R., Azizi M. *Ecotoxicol. Environ. Saf*., 2015, **120**:408

[4]. Govindaraju K., Tamil Selvan S., Kiruthiga V., Singaravelu G. *J. Biopesti*., 2010, **3**:394

[5]. Parashar U.K., Saxena P.S., Srivastava A. *Dig J Nano Biost*., 2009, **4**:166

[6]. Bar H., Bhui D.K., Sahoo G.P., Sarkar P., De S.P., Misra A. *Colloids. Surf. A*., 2009, **339**:139

[7]. Sondi I., Salopek-Sondi B. *J. Colloid. InterFace. Sci*., 2004, **275**:182

[8]. Logeshwar P., Silambarasan S., Abraham J. *J. Saudi chem. Soc*., 2012. **4**:45

[9]. Gardea–Torresdey J.L., Parson J.G., Gomez E., Peratta-Videa J., Troiani H.E., Santiago P., Yacaman M.J. *Nano. Lett.*, 2002, **2**:397

[10]. Tchoumbougnang F., Amvam Zollo P.H., Avlessi F., Alitonou G.A., Sohounhloue D.K., Ouamba J.M., Tsomambet A., Okemy–Andissa N., Dagne E., Agnaniet H., Bessiere J.M., Menut C. *J. Essent. Oil Res.,* 2006, **18**:199

[11]. Bilal A., Jahan N., Ahmed A., Bilal S.N., Habib S., HajraInt S. *J. Curr. Res. Rev*., 2012, **4**:83

[12]. Kaya I., Yigit N., Benli M. *Afr. J. Tradit, Complementary Altern. Med*., 2009, **5**:363

[13]. Benalla W., Bellahcen S., Bnouham M. *Curr. Diabetes Rev*., 2010, **6**:274

[14]. Dinesh kumar B., Analava Mitra M., Manjunatha A. *Int. J. Gre. Pharma*. 2010, **4**:121

[15]. Swarnalatha L., Rachel C., Ranjan S., Baradwaj P. Int. J. *Nanomater. Biostruct*., 2012, **2**:29

[16]. Elumalai E.K., Prasad T.N.V., Hemachandran J., Therasa D., Thirumalai T., David E. *J. Pharm. Sci. Res*., 2016, **2**:554

[17]. Rajan Rushender C., Madhavieerike M. *J. Pharm. Res*., 2012, **5**:3806

[18]. Shah A.T., Din M.L., Bashir S., Qadir M.A., Rashid F. *Analyt. Lett*., 2015, **48**:1180

[19]. Gao X., Zhang J., Zhang L. *Adv. Mate*. 2002, **14**:290

[20]. Xia D.Z., Yu X.F., Zhu Z.Y., Zou Z.D. *Nat. Prod. Res*., 2011, **25**:1893

[21]. Sun Y.P., Atorngitjawat P., Meziani M.J. *Langumuir*, 2001, **17**:5707

[22]. Shrivastava S., Dash D. *Nano. Micro. Letters*., 2010, **2**:168

[23]. Konishi K., Ohno K., Saitoh N., Nomura T., Nagamine S., Hishida H., Takahashi Y., Uruga T. *J. Biotechnol*., 2007, **128**:653

[24]. Nabikhan A., Kandasamy K., Raj A., Alikunhi N.M. *Colloids Surf. B: Biointerface.*, 2010, **79**:493

[25]. Sathyavathi R., Balamurali Krishna M., Venugoal Rao S., Saritha R., Narayana Rao D. *Adv. Sci. Lett*., 2010, **3**:6

[26]. Narayanan K.B., Sakthivel N. *Mater. Lett*., 2008, **62**:4590

[27]. Velayutham K., Raguman A.A., Rajakumar G., Roopan S.M., Elango G., Kamaraj C., Marimuthu S., Santhosh Kumar T., Iyappan M., Siva C. *Asian pac. J. Trop. Med*., 2013, **6**:101

[28]. Mandel S., Phadtare S., Sastry A. *Nano-micro Lett*., 2010, **2**:168

[29]. Balaji S.D., Basavaraja S., Deshpande R., Mahesh B.D., Prabahakar K.B., Venkataraman A. *Coll. Surf. B Bio*., 2009, **68**:92

[30]. Krishnaraj C., Jagan E.G., Rajasekar S., Kalaiselvam P.T., Mohan N. *Coll. Surf. B Bio..* 2010, **70**:56

[31]. Vivek R., Thangam R., Muthuselvan K., Gunasekaran P., Kaveri K., Kannan S. *Process Biochem*., 2012, **47**:2410

[32]. Xu H., Käll M. *Phys. Rev. Lett*., 2002, **989**:246802

[33]. Suman T.Y., Elumalai D., Kaleena P.K., Radhika Rajashree S.R. *Ind. Crops. Prod.*, 2013, **47**:245

[34]. Kaviya S., Sanathanalakshmi J., Viswananthan B., Muthumary J., Srivinasan K. *Spectro. Chemica. Acta Part A*., 2009, **79**:598

[35]. Shankar S.S., A Rai A., Ahma., Sastry M. *J. Col. Inter. Sci*., 2004, **275**:502

[36]. Kim K.J., Sung W.S., Moon S.K, Choi J.S., Kim J.G., Lee J.D. *J. Microbiol. Biotechnol*., 2008, **18**:1484

[37]. Sathishkumar M., Sneha K., Yun Y.S*. Biores.Technol*., 2010, **101**:7965

[38]. Liu Z., Buck nall D.G., Allen M.G. *Nanotechnology*., 2011, **22**:302

[39]. Priester J.H., Stoimenov P.K., Mielke R.E., Webb S.M., Ehrhardt C., Zhang J.P., Stucky G.D., Holden P.A. *Environ. Sci. Technol*., 2009, **43**:2589

How to cite this manuscript: Devan Elumalai, Manickam Sathiyaraj, Elangovan Vimalkumar, Patheri Kunyl Kaleena*, Maduraiveeran Hemavathi, Perumal Venkatesh. Bio fabricated of silver nanoparticles using *Ocimum basilicum* and its efficacy of antimicrobial and antioxidant activity. *Asian Journal of Green Chemistry*, 3(1) 2019, 103-124**.** DOI: 10.22034/ajgc.2018.6729